

Computational Models for Circadian Rhythms: Deterministic Versus Stochastic Approaches

Jean-Christophe Leloup, Didier Gonze,
and Albert Goldbeter

*Unité de Chronobiologie théorique, Faculté des
Sciences, Université Libre de Bruxelles, Brussels, Belgium*

Chapter 13

ABSTRACT

Circadian rhythms originate from intertwined feedback processes in genetic regulatory networks. Computational models of increasing complexity have been proposed for the molecular mechanism of these rhythms, which occur spontaneously with a period on the order of 24 h. We show that deterministic models for circadian rhythms in *Drosophila* account for a variety of dynamical properties, such as phase shifting or long-term suppression by light pulses and entrainment by light/dark cycles. Stochastic versions of these models allow us to examine how molecular noise affects the emergence and robustness of circadian oscillations. Finally, we present a deterministic model for the mammalian circadian clock and use it to address the dynamical bases of physiological disorders of the sleep/wake cycle in humans.

I. INTRODUCTION: THE COMPUTATIONAL BIOLOGY OF CIRCADIAN RHYTHMS

Most living organisms have developed the capability of generating autonomously sustained oscillations with a period close to 24 h. The function of these so-called *circadian rhythms* is to allow the organisms to adapt their physiology to the natural alternation of day and night. Circadian rhythms are endogenous because they can occur in constant environmental conditions (e.g., constant darkness). During the last two decades, experimental studies have shed much light on the molecular mechanism of circadian rhythms, which represents a long-standing problem in biology. In all eukaryotic organisms investigated so far, the molecular mechanism

of circadian oscillations relies on the negative feedback exerted by a clock protein on the expression of its gene (Hardin et al. 1990; Glossop et al. 1999; Lee et al. 2000; Alabadi et al. 2001; Reppert and Weaver 2002).

Even before details were known about their molecular origin, abstract mathematical models were used to probe the dynamic properties of circadian rhythms. A popular model of this type was provided by the van der Pol equations, which were originally proposed for sustained oscillations in electrical circuits. Thus, the van der Pol oscillator has been used for more than three decades for modeling circadian rhythms (e.g., to account for phase shifts of these rhythms by light pulses (Jewett and Kronauer 1998)). Another application involving this model pertains to modeling the enhanced fitness due to the resonance of circadian rhythms with the external light/dark cycle in cyanobacteria (Gonze et al. 2002c).

However, now that the molecular mechanism of circadian rhythms has largely been uncovered, mathematical models based on experimental observations have been proposed. Taking the form of a system of coupled ordinary differential equations, these deterministic models predict that in a certain range of parameter values the genetic regulatory network at the core of the clock mechanism can produce sustained oscillations of the limit cycle type. Deterministic models for circadian rhythms were first proposed for *Drosophila* and *Neurospora* (Goldbeter 1995, 1996; Leloup and Goldbeter 1998; Leloup et al. 1999; Smolen et al. 2001; Ueda et al. 2001), and later for mammals (Forger and Peskin 2003; Leloup and Goldbeter 2003, 2004; Becker-Weimann et al. 2004). The first model showing that oscillations can originate from negative feedback on gene expression was due to Goodwin (1965), who showed (already four decades ago) that periodic behavior may originate from such mode of genetic regulation. Modified versions of the Goodwin model are still being used to probe properties of circadian rhythms in organisms such as *Neurospora* (Ruoff et al. 2001). In this chapter we will focus on more recent models, which rely on more detailed molecular mechanisms.

One limitation of deterministic models is that they do not take into consideration the fact that the number of molecules involved in the regulatory mechanism within the rhythm-producing cells may be small as observed, for example, in *Neurospora* (Morrow et al. 1997). At low concentrations of protein or messenger RNA molecules, molecular fluctuations are likely to have a marked impact on circadian oscillations (Barkai and Leibler 2000). To assess the effect of molecular noise, it is necessary to resort to a stochastic approach. Comparing the predictions of deterministic and stochastic models for circadian rhythms shows that robust circadian oscillations can be observed even when the maximum number of mRNA and protein molecules is of the order of some tens and hundreds, respectively (Gonze et al. 2002a, 2002b, 2004a).

The goal of this chapter is to present an overview of deterministic and stochastic models for circadian rhythms. We will begin by presenting (in Section II) deterministic models for circadian oscillations of the PER protein and its mRNA in *Drosophila*. A core model will be presented, which also provides a useful model for circadian rhythms in *Neurospora*. This model for *Drosophila* circadian rhythms will

be extended to take into account the role of the TIM protein and the control of circadian behavior by light.

In Section III, we consider stochastic versions of these models. We examine how molecular noise affects the emergence of circadian oscillations and determine the influence of a variety of factors, such as number of protein and mRNA molecules, degree of cooperativity of repression, distance from bifurcation point, and rate constants characterizing the binding of the repressor protein to the gene. Two types of stochastic models are presented: one involves a fully detailed description of individual reaction steps, whereas a second relies on a non-developed description of nonlinear kinetic steps. Both types of models yield largely similar results. The study of stochastic models for circadian oscillations will allow us to characterize the domain of validity of deterministic models for circadian rhythms.

In Section IV we return to deterministic approaches and present a model for the mammalian circadian clock. We use this model to address the molecular bases of disorders of the sleep/wake cycle in humans, which are associated with dysfunctions of the clock. Computational models can thus be applied to investigating not only the molecular mechanism of circadian rhythms but the origin of associated physiological disorders. As discussed in Section V, the example of circadian rhythms illustrates how more and more complex models have been presented over the years to account for new experimental observations. We consider the need for such an increase in complexity of computational models for circadian rhythms, and the added insights these complex models provide for a better understanding of circadian behavior.

II. MODELING THE DROSOPHILA CIRCADIAN CLOCK

A. Overview of experimental observations

Some of the most remarkable advances in elucidating the molecular basis of circadian rhythms have been made in mutants of the fly *Drosophila* (Konopka 1979; Hall and Rosbash 1988; Baylies et al. 1993; Dunlap 1993), in which circadian rhythms affect the rest/activity cycle and the daily eclosion peaks of pupae. Both rhythms persist in constant darkness or temperature (Pittendrigh 1960). The classic work of Konopka and Benzer (1971) yielded *Drosophila* flies altered in their circadian system, owing to mutations in a single gene called *per* (for "period"). Four phenotypes were characterized: the wild type (per^+) has a free-running period of activity and eclosion close to 24 h; short-period mutants (per^s) have a period close to 19 h; in long-period mutants (per^l), the periodicity increases up to 29 h; and arrhythmic mutants (per^0) have lost the circadian pattern of eclosion or activity (Konopka and Benzer 1971; Konopka 1979). Interestingly, whereas in the wild type the period remains independent of temperature—a property known as temperature compensation, which is common to all circadian rhythms (Pittendrigh 1960)—the mutants per^l and per^s have lost this property (Konopka et al. 1989). In contrast to the wild

type, the period of their activity rhythm respectively increases and decreases with temperature. Accounting for temperature compensation of circadian rhythms remains an important challenge for computational biology.

A breakthrough for the mechanism of circadian rhythms in *Drosophila* was the finding (Hardin et al. 1990, 1992) that *per* mRNA is produced in a circadian manner. This periodic variation is accompanied by a circadian rhythm in the degree of abundance of PER. The peak in *per* mRNA precedes the peak in PER by 4 to 8 h (Zerr et al. 1990; Zeng et al. 1994). On the basis of this observation, Hardin et al. (1990, 1992) suggested that the *Drosophila* circadian rhythm results from a negative feedback exerted by the PER protein on the synthesis of the *per* mRNA. Post-translational modification of PER is also involved in the mechanism of circadian oscillations. Experimental evidence indeed indicates that PER is multiply phosphorylated (Edery et al. 1994). It appears that PER phosphorylation plays a role in the circadian oscillatory mechanism, by controlling the nuclear localization of PER and/or its degradation (Grima et al. 2002; Ko et al. 2002).

Overexpression of PER in *Drosophila* eyes represses *per* transcription and suppresses circadian rhythmicity in these cells, without affecting circadian oscillations in other *per*-expressing cells in the brain or the circadian rhythm in locomotor activity. This work shows that the action of PER on transcription is intracellular, and suggests that "each *per*-expressing cell contains an autonomous oscillator of which the *per* feedback loop is a component" (Zeng et al. 1994). Such a mechanism, based on negative autoregulation of transcription, has also been found in *Neurospora* (Aronson et al. 1994). The current view is that negative autoregulation of gene expression by a clock protein represents a unified mechanism for the generation of circadian rhythmicity in a wide variety of experimental systems (Dunlap 1999; Young and Kay 2001).

B. A core deterministic model for circadian oscillations of the PER protein and its mRNA

A first model for circadian oscillations in the *Drosophila* PER protein and its mRNA is based on multiple phosphorylation of PER and on the inhibition of *per* transcription by a phosphorylated form of the protein (Goldbeter 1995). This model, schematized in Figure 13.1a, can be viewed as a minimal core model because it takes into account a limited number of phosphorylated residues of PER. The model also applies to oscillations of FRQ and *frq* mRNA in *Neurospora*.

In the model, the *per* gene is first expressed in the nucleus and transcribed into *per* messenger RNA (mRNA). The latter is transported into the cytosol, where it is translated into the PER protein, P_0 , and degraded. The PER protein undergoes multiple phosphorylation, from P_0 into P_1 and from P_1 into P_2 . These modifications, catalyzed by a protein kinase, are reverted by a phosphatase. The fully phosphorylated form of the protein is marked up for degradation and transported into the nucleus in a reversible manner. The nuclear form of the protein (P_N) represses the transcription of the gene.

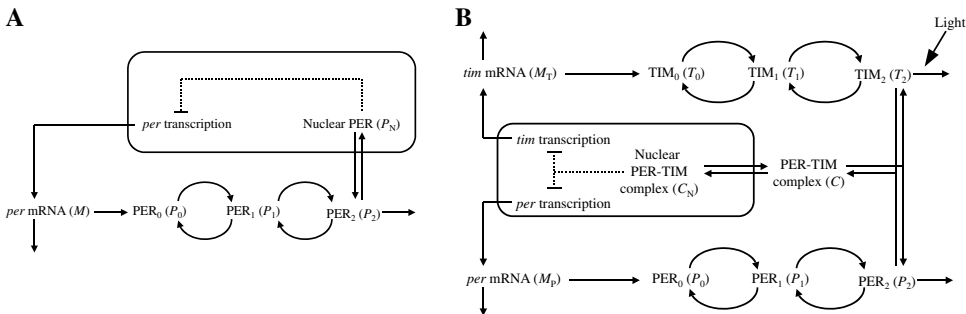


Figure 13.1. Schemes of the models for circadian oscillations in *Drosophila*. (a) The PER model is based on the sole negative regulation exerted by the PER protein on the expression of its gene (Goldbeter 1995). (b) The PER-TIM model incorporates the *tim* gene and its product, which forms a complex with the PER protein. This model is based on the negative regulation exerted by the PER-TIM complex on the expression of the *per* and *tim* genes. The effect of light is to increase the rate of TIM degradation (Leloup and Goldbeter 1998).

In the model, we consider two successive phosphorylations of PER, which is the minimal implementation of multiple phosphorylation. A single phosphorylation step would yield similar results. In fact, sustained oscillations can occur in the absence of phosphorylation, as shown by the study of a three-variable model representing an even simpler model for circadian oscillations (Leloup et al. 1999; Gonze and Goldbeter 2000; Gonze et al. 2000). We nevertheless focus on a model that includes multiple phosphorylation, because this process contributes to the mechanism of circadian oscillations by introducing a delay in the negative feedback loop.

In the model, the temporal variation of the concentrations of mRNA (M) and of the various forms of the regulatory protein—cytosolic (P_0, P_1, P_2) or nuclear (P_N)—is governed by the following system of kinetic equations (see Goldbeter (1995, 1996) for further details):

$$\begin{aligned}
 \frac{dM}{dt} &= v_s \frac{K_I^n}{K_I^n + P_N^n} - v_m \frac{M}{K_m + M} \\
 \frac{dP_0}{dt} &= k_s M - v_1 \frac{P_0}{K_1 + P_0} + v_2 \frac{P_1}{K_2 + P_1} \\
 \frac{dP_1}{dt} &= v_1 \frac{P_0}{K_1 + P_0} - v_2 \frac{P_1}{K_2 + P_1} - v_3 \frac{P_1}{K_3 + P_1} + v_4 \frac{P_2}{K_4 + P_2} \\
 \frac{dP_2}{dt} &= v_3 \frac{P_1}{K_3 + P_1} - v_4 \frac{P_2}{K_4 + P_2} - v_d \frac{P_2}{K_d + P_2} - k_1 P_2 + k_2 P_N \\
 \frac{dP_N}{dt} &= k_1 P_2 - k_2 P_N
 \end{aligned}
 \tag{13.1}$$

In these equations, the phosphorylation and dephosphorylation terms (with maximum rates v_1, v_3 , and v_2, v_4 , respectively)—as well as the degradation terms for

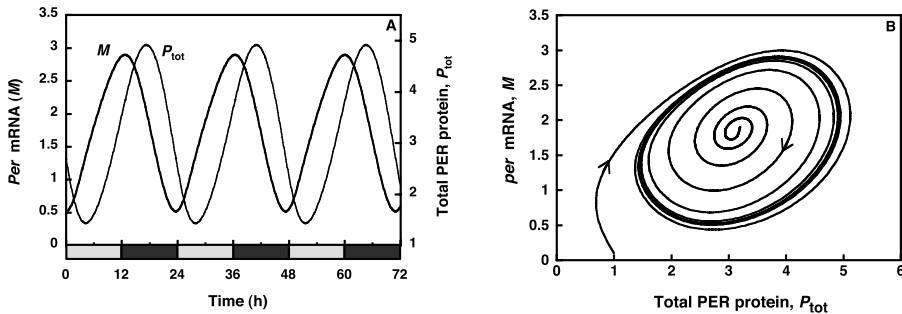


Figure 13.2. Sustained oscillations and limit cycle generated by the PER model. (a) Temporal variation in *per* mRNA (M) and in the total amount of PER protein (P_{tot}). (b) Sustained oscillations in total PER protein and *per* mRNA (expressed in nM) correspond to the evolution toward a limit cycle when the system's trajectory is projected onto the (M , P_{tot}) plane. Starting from two different initial conditions, the system reaches a unique closed curve characterized by a period and amplitude that are fixed for the given set of parameter values. The curves have been obtained by numerical integration of Equations 13.1. Parameter values are $v_s = 0.76$ nM/h, $v_m = 0.65$ nM/h, $k_s = 0.38$ h⁻¹, $v_d = 0.95$ nM/h, $k_1 = 1.9$ h⁻¹, $k_2 = 1.3$ h⁻¹, $K_1 = 1$ nM, $K_d = 0.2$ nM, $K_1 = K_2 = K_3 = K_4 = 2$ nM, $n = 4$, $V_1 = 3.2$ nM/h, $V_2 = 1.58$ nM/h, $V_3 = 5$ nM/h, and $V_4 = 2.5$ nM/h. Initial conditions are $M = 0.1$, $P_0 = P_1 = P_2 = P_N = 0.25$ ($P_{\text{tot}} = 1$), $M = 1.9$, and $P_0 = P_1 = P_2 = P_N = 0.8$ ($P_{\text{tot}} = 3.2$) (see Goldbeter (1995, 1996)).

mRNA and fully phosphorylated PER protein (with maximum rates v_m and v_d , respectively)—are all of Michaelian form corresponding to non-cooperative enzyme kinetics. The repression term takes the form of a Hill equation characterized by the Hill coefficient n . Repression by P_N becomes steeper and steeper as the degree of cooperativity n increases above unity. Although higher cooperativity favors the occurrence of sustained oscillations, periodic behavior can also be obtained for $n = 1$ (i.e., in the absence of cooperativity in repression).

For an appropriate set of parameter values, the model accounts for the occurrence of sustained oscillations in continuous darkness (Figure 13.2a). When plotting the time evolution of one variable (e.g., *per* mRNA (M)) as a function of another variable (e.g., the total amount of PER protein (P_{tot})), these oscillations correspond in such a phase plane to the evolution toward a closed curve, known as a limit cycle (Figure 13.2b). This name stems from the fact that the same closed trajectory is reached regardless of initial conditions, as illustrated in Figure 13.2b. In addition to accounting for the circadian rhythms in mRNA and for protein level, the model shows how variations in parameters such as the rate of degradation of PER or the rate of its translocation into the nucleus may change the period of the oscillations, or even suppress rhythmic behavior (Goldbeter 1995, 1996).

When the model based on PER alone was proposed, the way light affects circadian rhythms in *Drosophila* was still unknown. In 1996, a series of papers showed, concomitantly, that a second protein—TIM (for TIMELESS)—forms a complex with PER, and that light acts by inducing degradation of TIM (Hunter-Ensor et al. 1996; Lee et al. 1996; Myers et al. 1996; Zeng et al. 1996). These observations paved the

way for the construction of a more detailed computational model incorporating the formation of a PER-TIM complex as well as the enhancement of TIM degradation during the light phase.

C. A ten-variable deterministic model for circadian oscillations in *Drosophila*

The ten-variable model for circadian oscillations of the PER and TIM proteins and of *per* and *tim* mRNAs in *Drosophila* (Leloup and Goldbeter 1998; Leloup et al. 1999) is schematized in Figure 13.1b. The mechanism is based on the negative feedback exerted by the complex between the nuclear PER and TIM proteins on the expression of their genes. For each of these proteins, transcription, translation, and multiple phosphorylation are treated as in the PER model of Figure 13.1a. The fully phosphorylated proteins PER and TIM are marked up for degradation, and form a complex that is transported into the nucleus in a reversible manner. The nuclear form of the PER-TIM complex represses the transcription of the *per* and *tim* genes.

Recent experiments indicate that repression is in fact of indirect nature: a complex between two activators, the CLOCK and CYC proteins, promotes the expression of the *per* and *tim* genes. The PER-TIM complex prevents this activation by forming a complex with CLOCK and CYC (Darlington et al. 1998; Rutila et al. 1998; Lee et al. 1999). We return to the effect of such an indirect negative feedback in Section IV, restricting the present discussion to the PER-TIM model. In this model, the variables are the concentrations of the mRNAs (M_P and M_T), the various forms of the PER and TIM proteins ($P_0, P_1, P_2, T_0, T_1, T_2$), and the cytosolic (C) and nuclear (C_N) forms of the PER-TIM complex. The temporal evolution of the concentration variables is governed by the following system of 10 kinetic equations (see Leloup and Goldbeter (1998) and Leloup et al. (1999) for further details):

$$\begin{aligned}
 \frac{dM_P}{dt} &= v_{sP} \frac{K_{IP}^n}{K_{IP}^n + C_N^n} - v_{mP} \frac{M_P}{K_{mP} + M_P} - k_d M_P \\
 \frac{dP_0}{dt} &= k_{sP} M_P - V_{1P} \frac{P_0}{K_{1P} + P_0} + V_{2P} \frac{P_1}{K_{2P} + P_1} - k_d P_0 \\
 \frac{dP_1}{dt} &= V_{1P} \frac{P_0}{K_{1P} + P_0} - V_{2P} \frac{P_1}{K_{2P} + P_1} - V_{3P} \frac{P_1}{K_{3P} + P_1} + V_{4P} \frac{P_2}{K_{4P} + P_2} - k_d P_1 \\
 \frac{dP_2}{dt} &= V_{3P} \frac{P_1}{K_{3P} + P_1} - V_{4P} \frac{P_2}{K_{4P} + P_2} - k_3 P_2 T_2 + k_4 C - v_{dP} \frac{P_2}{K_{dP} + P_2} - k_d P_2 \\
 \frac{dM_T}{dt} &= v_{sT} \frac{K_{IT}^n}{K_{IT}^n + C_N^n} - v_{mT} \frac{M_T}{K_{mT} + M_T} - k_d M_T \\
 \frac{dT_0}{dt} &= k_{sT} M_T - V_{1T} \frac{T_0}{K_{1T} + T_0} + V_{2T} \frac{T_1}{K_{2T} + T_1} - k_d T_0 \\
 \frac{dT_1}{dt} &= V_{1T} \frac{T_0}{K_{1T} + T_0} - V_{2T} \frac{T_1}{K_{2T} + T_1} - V_{3T} \frac{T_1}{K_{3T} + T_1} + V_{4T} \frac{T_2}{K_{4T} + T_2} - k_d T_1
 \end{aligned} \tag{13.2}$$

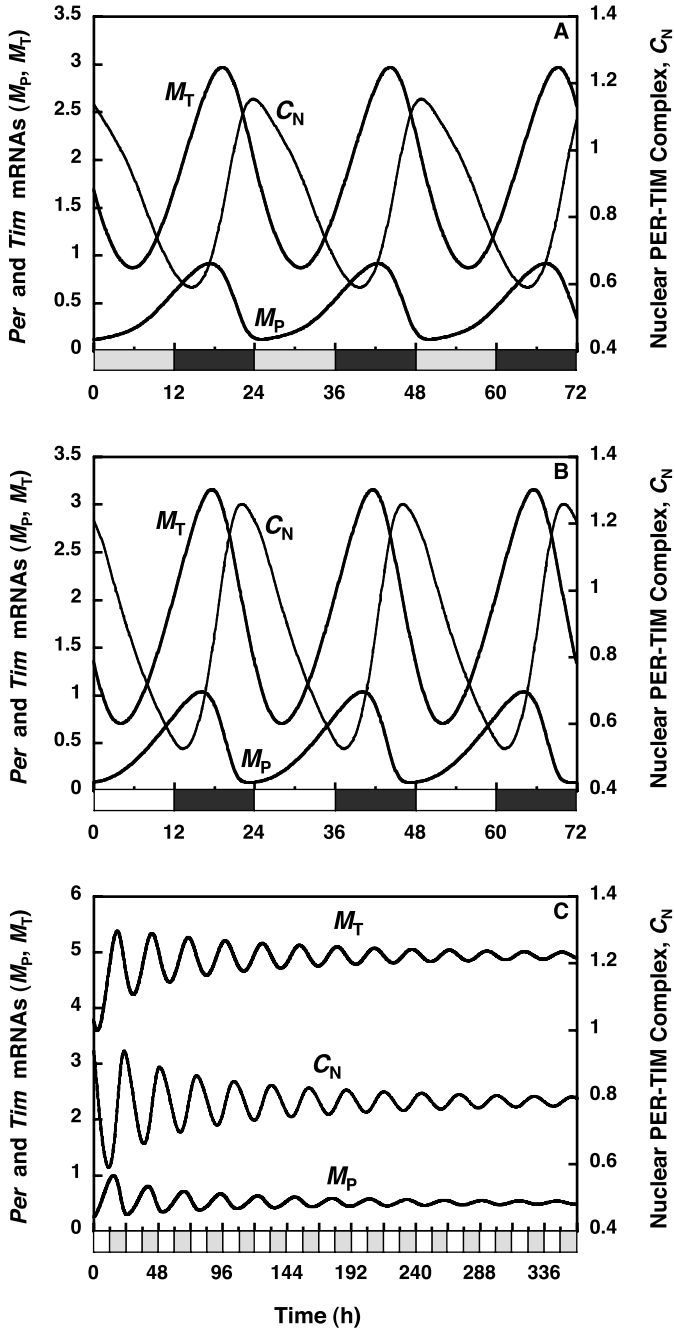
$$\begin{aligned}\frac{dT_2}{dt} &= V_{3T} \frac{T_1}{K_{3T} + T_1} - V_{4T} \frac{T_2}{K_{4T} + T_2} - k_3 P_2 T_2 + k_4 C - v_{dT} \frac{T_2}{K_{dT} + T_2} - k_d T_2 \\ \frac{dC}{dt} &= k_3 P_2 T_2 - k_4 C - k_1 C + k_2 C_N - k_{dC} C \\ \frac{dC_N}{dt} &= k_1 C - k_2 C_N - k_{dN} C_N\end{aligned}$$

These equations correspond to one particular version in a family of possible models, which differ by details of the molecular implementation of the feedback mechanism. Thus, rather than considering the formation of a complex between the fully phosphorylated forms of PER and TIM the complex could be made also (or instead) between the non-phosphorylated or mono-phosphorylated forms of the proteins. These other versions of the basal model yield largely similar results.

The various terms appearing in Equations 13.2 are similar to those of Equations 13.1. We have added nonspecific degradation terms, characterized by the rate constants k_d , k_{dC} , and k_{dN} . These linear terms are generally of negligible magnitude, and are not essential for oscillations. Their inclusion ensures the existence of a steady state when the specific protein degradation processes are inhibited. In Equations 13.2, parameter v_{dT} represents the maximum value of the TIM degradation rate. This is the light-sensitive parameter, which will be set to a constant low value during continuous darkness, and to a constant high value during continuous light. In a light/dark cycle, v_{dT} will vary in a square-wave manner between these two extreme values. The square-wave corresponds well to laboratory conditions under which light varies in an all-or-none manner. The natural variation of light is of course smoother, and other waveforms should be considered to address the effect of variations of luminosity under natural light/dark cycles.

Much as the PER model, the model based on the formation of the PER-TIM complex can account for sustained autonomous oscillations originating from negative auto-regulatory feedback. Now, however, we may address the dynamic behavior of the model in various lighting conditions, by incorporating suitable changes in parameter v_{dT} . Thus, as illustrated in Figure 13.3, sustained oscillations can occur

Figure 13.3. Circadian oscillations in the PER-TIM model. From top to bottom, the curves correspond to (a) sustained oscillations in continuous darkness, (b) entrainment by a light/dark cycle of 24 h period (12 : 12 LD), and (c) damped oscillations in continuous light. The LD cycle is symbolized by the alternation of white and black bars. Continuous darkness is symbolized by the alternation of gray and black bars. Shown is the temporal variation in *per* and *tim* mRNAs (M_p , M_t) and in the concentration of nuclear PER-TIM complex (C_N). The curves have been obtained by numerical integration of Equations 13.2 (Leloup and Goldbeter 1998). Parameter values are $v_{sp} = 0.8 \text{ nM h}^{-1}$, $v_{sT} = 1 \text{ nM h}^{-1}$, $v_{mp} = 0.8 \text{ nM h}^{-1}$, $v_{mT} = 0.7 \text{ nM h}^{-1}$, $K_{mp} = K_{mT} = 0.2 \text{ nM}$, $k_{sp} = k_{sT} = 0.9 \text{ h}^{-1}$, $v_{dp} = v_{dT} = 2 \text{ nM h}^{-1}$, $k_1 = 1.2 \text{ h}^{-1}$, $k_2 = 0.2 \text{ h}^{-1}$, $k_3 = 1.2 \text{ nM}^{-1} \text{ h}^{-1}$, $k_4 = 0.6 \text{ h}^{-1}$, $K_{IP} = K_{IT} = 1 \text{ nM}$, $K_{dP} = K_{dT} = 0.2 \text{ nM}$, $n = 4$, $K_{1P} = K_{1T} = K_{2P} = K_{2T} = K_{3P} = K_{3T} = K_{4P} = K_{4T} = 2 \text{ nM}$, $k_d = k_{dC} = k_{dN} = 0.01 \text{ h}^{-1}$, $V_{1P} = V_{1T} = 8 \text{ nM h}^{-1}$, $V_{2P} = V_{2T} = 1 \text{ nM h}^{-1}$, $V_{3P} = V_{3T} = 8 \text{ nM h}^{-1}$, and $V_{4P} = V_{4T} = 1 \text{ nM h}^{-1}$. Parameter v_{dT} is increased from 2 nM/h in the dark phase to 5 nM/h in the light phase (Leloup and Goldbeter 1998).



in continuous darkness (DD), but damped oscillations occur in conditions corresponding to continuous light (LL), as observed in *Drosophila* (Qiu and Hardin 1996). In LL, the light-sensitive parameter was chosen so that it takes a high value corresponding to a stable steady state. The disappearance of oscillations can be explained intuitively: because of enhanced degradation, the TIM protein cannot reach a level allowing effective repression by the PER-TIM complex. Oscillations observed in DD with a period close to 24 h can be entrained by a 12 : 12 LD cycle (12 h of light followed by 12 h of darkness). Experimentally, there exists a window of entrainment, ranging typically from 21 to 28 h (Moore-Ede et al. 1982).

The PER-TIM model allows us to compare theoretical predictions with experimental observations in a variety of cases. A first comparison pertains to entrainment by LD cycles of varying photoperiod. As shown by the experiments of Qiu and Hardin (1996), the peak in *per* mRNA always follows the transition from the L to the D phase by about 4 h. A similar result is obtained in the PER-TIM model (Figure 13.4). The lag after the L to D transition appears to be the same regardless of the duration of the light phase, because the level of TIM has decreased to a minimum value at the end of the L phase, and the time required for the PER-TIM complex to accumulate during the dark phase above the threshold for repression remains unchanged.

Another key comparison pertains to the phase shifts induced by light pulses in continuous darkness. Depending on the phase at which these perturbations are made, circadian oscillations can be either advanced or delayed. Alternatively, no phase shift may occur. These data yield a phase response curve (PRC) when the phase shift is plotted as a function of the phase of perturbation. The PRC is an

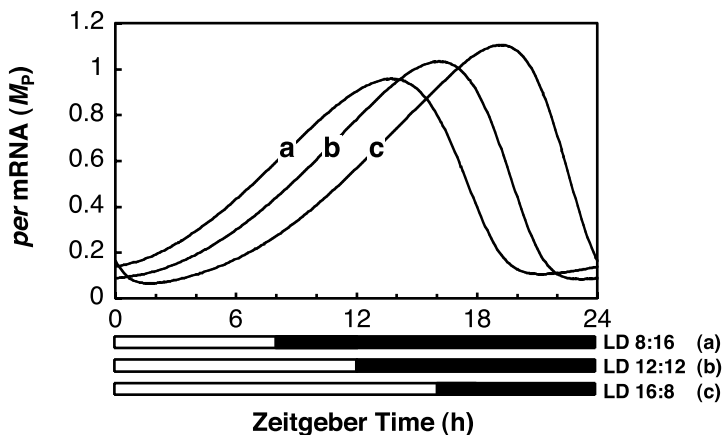


Figure 13.4. Phase locking of the *per* mRNA oscillations in the PER-TIM model. The three curves correspond to entrainment by a light/dark cycle of 24 h period but with different photoperiod: (a) 8 : 16 LD cycle, (b) 12 : 12 LD cycle, and (c) 16 : 8 LD cycle. The LD cycles are symbolized by the alternation of white and black bars. The curves have been obtained by numerical integration of Equations 13.2. Parameter values are as in Figure 13.3.

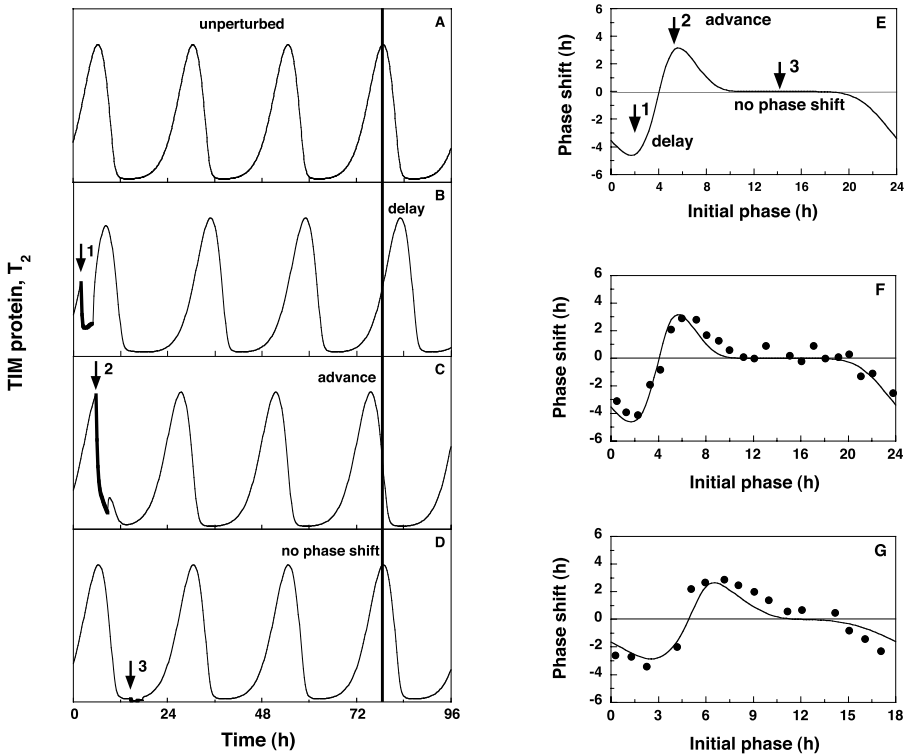


Figure 13.5. Phase shifting by a light pulse comparison with experiments. (a) Unperturbed oscillations of phosphorylated TIM (T_2). The vertical line through the fourth peak serves as reference for determining phases shifts. (b–d) Transient perturbations at three different phases of the oscillations, producing, respectively, a phase delay, a phase advance, or an absence of phase shift. The arrows mark the beginning of the light pulse and the thick lines indicate both the duration and the effect of this perturbation (see following). (e) Phase response curve (PRC) obtained by plotting the phase shift as a function of the phase at which the perturbation is applied. The perturbation takes the form of a 3-h twofold increase in TIM maximum degradation rate (v_{dT}), triggered by the light pulse. (f and g) PRCs obtained theoretically (solid lines) for the wild type (panel F) and for the *per^S* mutant (panel G) in *Drosophila*. The theoretical predictions compare well with the experimental observations (dots) based on data obtained by Konopka and Orr using a 1-min light pulse (redrawn from Figure 2 of Hall and Rosbash (1987)). The oscillations of the TIM protein (panels A– through D) and the PRCs (panels E through G) have been obtained by numerical integration of Equations 13.2 (Leloup and Goldbeter 1998). Parameter values are listed in Figure 2 of Leloup and Goldbeter (1998). For the PRCs, the zero phase is chosen, as in the experiments (Hall and Rosbash 1987), so that the minimum in *per* mRNA occurs after 12 h.

important tool in the study of circadian rhythms. We may simulate the effect of light pulses in the PER-TIM model by transiently increasing the maximum rate of TIM degradation, v_{dT} . Unperturbed oscillations of fully phosphorylated TIM (T_2) are shown in Figure 13.5a, where the vertical line through the fourth peak will serve as reference for determining phase shifts triggered by transient perturbations.

As shown in Figure 13.5b, when the perturbation is applied during the rising phase of TIM a phase delay is observed. In contrast, a phase advance occurs when the perturbation is made at the maximum of TIM (Figure 13.5c), whereas no phase shift is observed when the pulse is given at the minimum of TIM (Figure 13.5d). The latter result stems from the fact that when TIM is already at its minimum a transient increase in TIM degradation remains without effect. Plotting the phase shifts as a function of the phase of perturbation yields the PRC shown in Figure 13.5e, where the arrows 1 through 3 refer to the situations depicted in panels B through D, respectively. The predictions of the model compare well with the experimental PRC both for wild-type flies (Figure 13.5f, where the solid curve is the same PRC as in panel E) and for the *per^s* mutant (Figure 13.5g). The model indicates that the dead zone in which no phase shift occurs is nearly absent in the *per^s* mutant because TIM remains near its minimum for a relatively much shorter time, as a result of the faster degradation of PER in this mutant (see Figure in Leloup and Goldbeter (1998)).

Obtaining good agreement with experimental observations is not straightforward, as this requires an appropriate characterization of the biochemical effects of a light pulse on the circadian clock. In constructing the theoretical PRC of Figure 13.5, we assumed that the effect of the light pulse is to double during 3 h the maximum rate of TIM degradation. Other combinations of multiplication factor and duration of increase may also yield satisfactory agreement. The interest of this result is to predict that the light pulse should have long-lasting biochemical consequences that may outlast the light pulse itself. This prediction is in fact corroborated by recent experimental observations (Busza et al. 2004).

Other results obtained with the PER-TIM model are of a more counter-intuitive nature. First, the model shows that in a certain range of parameter values sustained oscillations of the limit cycle type may coexist with a stable steady state. Such a situation, known as hard excitation, provides a possible explanation for the suppression of circadian rhythms by a single light pulse and for the subsequent restoration of periodic behavior by a second such pulse. This puzzling phenomenon, which has been observed in a variety of organisms, remains largely unexplained. The model indicates that over a range of phases corresponding to TIM increase in *Drosophila* transient increases in parameter v_{dT} may bring the system from the limit cycle into the basin of attraction of the stable steady state. A second pulse in v_{dT} may then bring back the oscillations (Figure 13.6a). Suppression is only possible over a finite portion of the limit cycle, as shown in Figure 13.6b. The characteristics (duration and amplitude) of the suppressing pulse change with the phase of perturbation in this domain (Leloup and Goldbeter 2001). In contrast, a single critical perturbation suppressing the rhythm exists in the situation described by Winfree (1980), wherein the stable limit cycle surrounds an unstable steady state. However, suppression is only transient in that case. The coexistence between a stable steady state and a stable limit cycle (illustrated in Figure 13.6a) is by no means uncommon, but a computational model is clearly needed to predict the occurrence of such a phenomenon.

We were at first surprised to observe that the deterministic PER-TIM model was also capable of producing chaotic behavior in constant environmental conditions

